EFFECT OF CHROMINIUM DOPING ON STRUCTURAL, MORPHOLOGICAL AND OPTICAL STUDY OF ZINC OXIDE NANOPARTICLES BY CO-PRECIPITATION TECHNIQUE

L. H. Kathwate[1], M. B. Awale[1], S. D. Lokhande[1], Y. S. Sudake[2] S.P. Kamble[3] V. D. Mote[1]*

[1]*Thin Films and Materials Science Research Laboratory, Department of Physics, Dayanand Science College, Latur – 413 512, Maharashtra, India*
[2]*Dept. of Physics, New Arts, Commerce and Science College Shevgaon414502*
3Dept. of Physics, C.T Bora CollegeShirur-412210
Corresponding author e-mail id: vmote.physics@gmail.com

Abstract

Undoped and Chrominium (Cr) doped Zinc oxide (ZnO) nanoparticles have been synthesized by novel co-precipitation route. Their structural, morphological and optical properties of pure and Cr doped ZnO nanoparticles have been studied using X-ray diffraction (XRD), Transmission electron microscope (TEM) UV-VIS techniques. Polycrystalline nature with hexagonal (wurtzite) crystal structure of undoped and Cr doped ZnO samples was confirm using XRD patterns. The measurement results of X-ray diffraction (XRD) show that the lattice parameters of $Zn_{1-x}Cr_xO$ nanoparticles decreases with the increase of Cr content, implying that Cr^{3+} is substituted into Zn^{2+} site. TEM images confirm that the prepared samples have nanocrystalline in nature. The mean crystallite size calculated by Debye-Scherrer formula was in the range of 17 – 23 nm and strain increases with increasing Cr doping of Cr doped ZnO nanoparticles. The absorption spectra at room temperature exhibit that the band gap of the Cr-doped ZnO nanoparticles decreases with the Cr concentration, illustrating that the modulation of band gap is caused by Cr addition.

Keywords: Nanoparticles; chemical analysis; spintronics; ZnO; bond length; optical properties.

I. Introduction

Dilute magnetic semiconductors (DMSs) are promising materials candidate for next generation spintronics devices because of the possibility of seamlessly integrating DMS into current semiconductor technology [1]. ZnO is a wide-band gap semiconductor with a direct band gap energy of 3.37 eV and exciton bounding energy of 60 meV, which is much larger than that of ZnSe (22 meV) and GaN (25 meV). In this regard, ZnO has attracted considerable attention because of great potential application like photo catalysis, gas sensors, varistors, low-voltage phosphor materials, solar cells and optoelectronic devices [2 - 7].

Cr is an important transition metal element and it has close ionic radius parameter to that of Zn^{2+}, which means that Cr^{3+} can easily penetrate into ZnO crystal lattice or substitute Zn^{2+} position in crystal [8]. Recently, many researchers have reported the formation of $Zn_{1-x}TM_xO$ nanostructures with different methods such as thermal hydrolysis technique [9], spray pyrolysis [10], chemical vapour deposition [11], thermal evaporation of ZnO [12], hydrothermal syntheses [13, 14], low temperature wet-chemical reaction [15].

However, there are few reports on Cr-doped ZnO nanoparticles were prepared by chemical technique. In comparison with other equipments, the chemical technique has many advantages in the preparation of $Zn_{1-x}Cr_xO$ nanoparticles, such as low cost and low temperature. The high temperature can produce the high crystal quality of $Zn_{1-x}Cr_xO$ nanoparticles and make Cr dopant diffuse well into the base compound. These nanoparticles have reduced energy band gap and a potential application for the window material for solar cells. Therefore, it is necessary to investigate the fabrication of $Zn_{1-x}Cr_xO$ nanoparticles.

In this paper, we report that the different morphologies of Cr- doped ZnO nanoparticles were synthesized by a simple chemical technique. The results indicate that the Cr doping plays a crucial role on controlling the morphologies, structural and optical properties of $Zn_{1-x}Cr_xO$ nanoparticles.

II. EXPERIMENTAL DETAILS

Chemicals used

To synthesis of pure and Cr doped ZnO nanoparticles, the zinc acetate dehydrate (99.99% purity) $Zn(CH_3COO)_2.2H_2O$, Chromonium acetate (99.99% purity) $Cr(CH_3COO)_2.6H_2O$, KOH, Methanol, Ethanol were purchased from M/s Sigma Merck Limited, India. All chemicals were of analytical reagent grade (AR) and were directly used without any special treatment.

Synthesis procedure

Samples with compositional formula of $Zn_{1-x}Cr_xO$, with x = 0.00, 0.05 and 0.10 were prepared by co-precipitation route in an alcoholic medium (methanol). In this procedure, to prepare pure ZnO, Zinc acetate dehydrate was dissolved in methanol (100 ml) and other containing NaOH in methanol (100 ml) were prepared and added both by constant magnetic stirring while heating at 285 K for 2 h. The precipitate separated from the solution by filtration, washed several times with distilled water and ethanol then dried in air at 400 K to obtain ZnO nanoparticles. The samples obtained were annealed at 683 K in air for 8 h. To synthesis Cr doped (0 to 10%) ZnO nanoparticles, Zinc acetate dehydrate and Cr acetate tetrahydrate were dissolved in methanol (100 ml) and other containing of NaOH in methanol (100 ml) were prepared and added by constant magnetic stirring while heating at 285 K for 2 h. The precipitate separated from the solution by filtration, washed several times with distilled water and ethanol then dried in air at 400 K. The samples obtained were annealed in air for 8 h at 683 K.

Characterization

The crystalline structure, phase purity and size of the pure and Cr doped ZnO nanoparticles were determined by X-ray diffraction (XRD) using X-ray diffractometer (Model: PW-3710) employing Cuk_α (λ = 1.5406 A^o) radiation, operating at 40 kV and 40 mA, in the 2θ range 20-80^0 with a scanning step of 0.02^0 and analyzed by comparing with the standard JCPDS cards (JCPDS No.36-1451). To study the sample morphology, the powders were ultrasonically mixed with ethanol and suspended on a Cu mesh, which is the sample holder of transmission electron microscope (TEM) operated at 200 kV(TEM- Model CM 200, SUPERTWIN). Absorption spectra were recorded using Uv-Vis spectrometer (JASCO) in the wavelength range 200–800 nm with a step of 2 nm.

III. RESULTS AND DISCUSSION

a. Structural study

The XRD diffraction patterns for pure and Cr doped ZnO nanoparticles are shown in figures 1(a) & 1(b). The XRD patterns showed that the nanoparticles were polycrystalline in nature, with hexagonal crystal structure and in agreement with JCPDS 36-1451. The positions were indexed to the (100), (002), (101), (102), (110), (103), (200), (112), (201), (004) and (202) crystallographic planes, and the peak position were determine to be consistent with JCPDS card. The peaks position angle of Cr doped ZnO are shifted to the lower angle of ZnO crystal indicated that Cr ions were substituted lodged in the ZnO lattice. No extra peaks related to crystal phases of Cr metal clusters were found which confirmed that the doping level within the solubility limit.

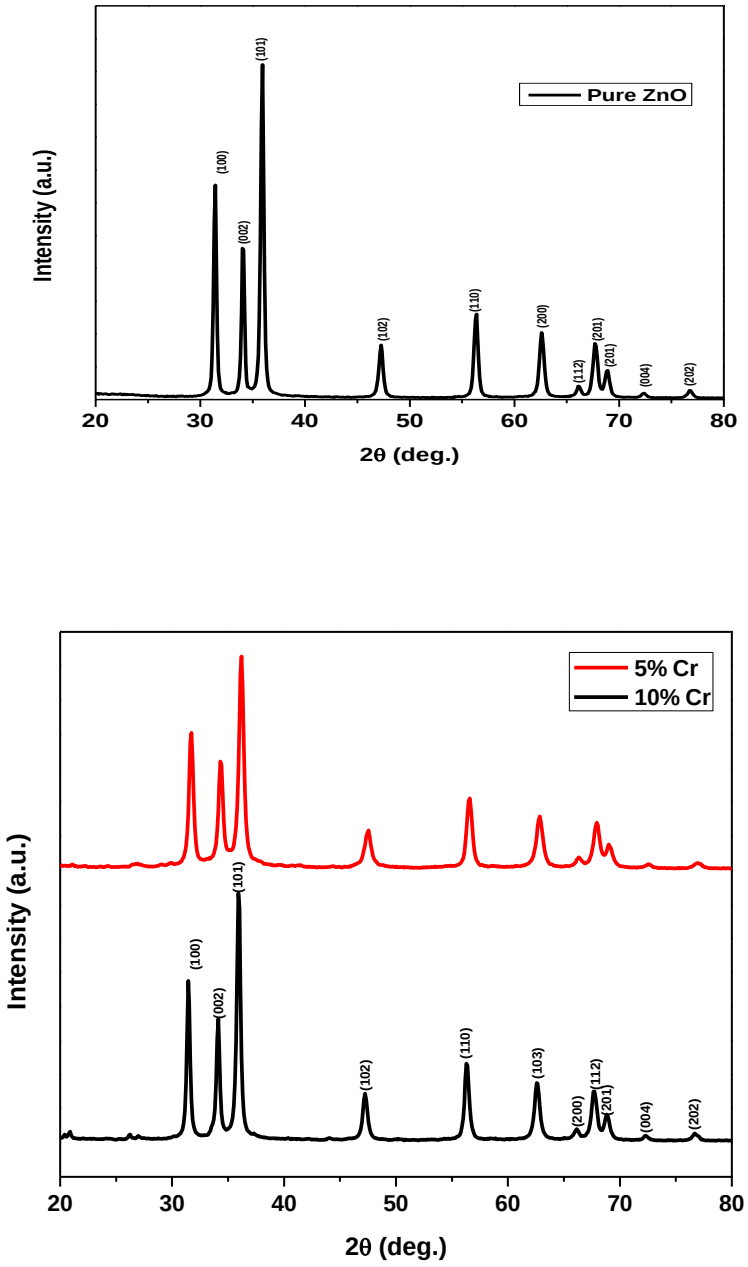

Fig. 1 XRD patterns of the undoped and Cr doped ZnO nanoparticles.

The lattice parameters of the obtained nanoparticles are calculated from the following relation:

$$\sin^2\theta = \frac{\lambda^2}{4a^2}\left[\frac{4}{3}(h^2+hk+k^2)+\frac{a^2l^2}{c^2}\right] \qquad (1)$$

where a & c are lattice parameters, θ is the Bragg's angle of the peaks, (hkl) are Mirrer Indices, λ is the wavelength of x-ray radiation. The lattice parameters a & c are determined the (100) and (002) planes respectively as follows:

$$a = \frac{\lambda}{\sqrt{3}\sin\theta} \quad (2)$$

$$c = \frac{\lambda}{2\sin\theta} \quad (3)$$

From the investigation of lattice parameters values as shown in table 1, it can be seen that the lattice parameters goes on decreasing with increasing Cr content in Zn, it may be due to the small ionic radii of Cr^{3+} as compared to the Zn^{2+}.

The volume is determined from XRD data using well known formula:

$$V = 0.866 \times a^2 \times c \quad (4)$$

The calculated volume of unit cell in our case decreased with increase in Cr doping. The reduction of volumes of Cr doped ZnO nanoparticles which may be attributed to the evidences of lattice parameters in Cr doped ZnO nanoparticles. Table 1 gives the u parameter, bond length and c/a ratio for undoped and Cr doped ZnO nanoparticles. From these results, it was clear that the u parameter, bond length and c/a ratio were also decreased with increasing Cr doping content.

The average crystallite size of the nanocrystals was calculated from x- ray line broadening of the diffraction peaks using Scherrer's formula,

$$D = \frac{k\lambda}{\beta_D \cos\theta} \quad (5)$$

where D is crystalline size, K is shape factor (0.9), λ is wavelength of Cukα radiation, β_D is instrumental corrected integral breadth of the reflection (in radians) located at 2θ and θ is angle of reflection (in degree) was utilized to relate the crystalline size of the line broadening. The results are sented in table 2. It is observed that the average crystallite size was changing with increasing Cr doping in ZnO samples. This may be attributable to the small grain growth of pure ZnO as compared to Cr doped ZnO samples. The Cr doped ZnO nanoparticles prepared was by using low temperature Co-precipitation route. In addition, result shown that the samples have a single phase hexagonal crystal structure with decreasing crystalline size with increasing Cr content.

The Wilson [16] pointed that the integral breadth (β_ε) arising from isotropic strain is related to the integral breadth of the strain distribution (ε) is

$$\beta_\varepsilon = C\varepsilon \tan\theta \quad (6)$$

Where C is proportional constant to convert into the strain. The C = 4 which is corresponding to maximum of strain [17-18].

$$\varepsilon = \frac{\beta_{hkl}}{4\tan\theta} \quad (7)$$

The average crystallite size and strain are given in table 1. From table, it can be seen that, average crystallite decrease and strain increase with increasing Cr doping in ZnO samples. Based on this study, it confirms that Cr surly substituting ZnO lattice.

Table 1. Lattice parameters, volume, u parameter, bond length, c/a ratio, average crystallite size and strain of undoped and Cr doped ZnO nanoparticles.

Sr. no.	Samples	Lattice parameters		Volume V (A°)	u	L (A°)	c/a ratio	D (nm)	ε
		a (A°)	c (A°)						
1.	**ZnO**	3.2697	5.2396	48.5131	0.37981	1.99007	1.6024	21.81	0.001625
2.	**5% Cr**	3.2682	5.2375	48.4478	0.37979	1.9892	1.6025	22.93	0.001576
3.	**10% Cr**	3.2529	5.2116	47.7566	0.37986	1.9797	1.6021	20.59	0.001824

b. Morphological study

Fig. 2 (a & b) shows the TEM images of pure and 10% Cr doped ZnO nanoparticles. ZnO image consisting of hexagonal like shape with the particle size of 28-31 nm was observed. The increase in the Cr content lead to reduction in the particles size and spherical like shape was observed. These result suggest that formation of nanocrystalline structure with particles size in ihte range of 16-31 nm.

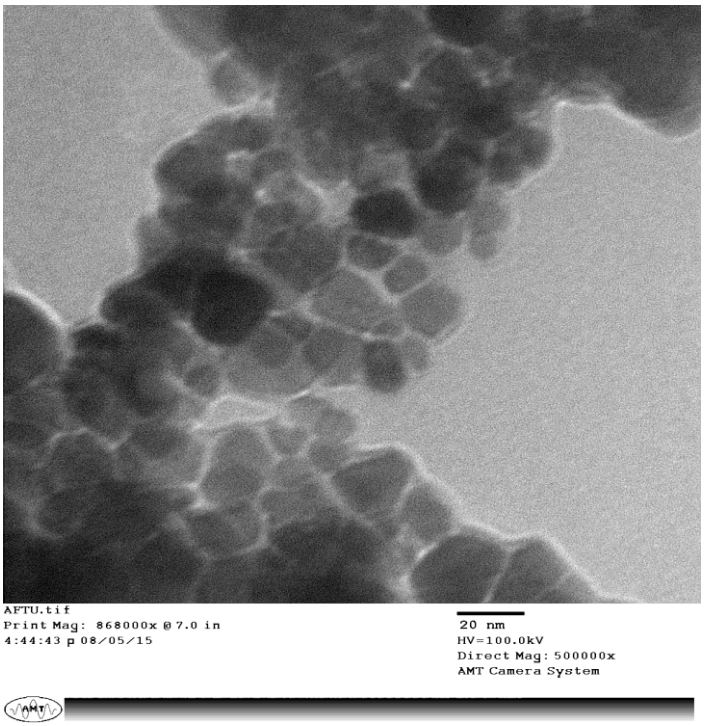

Fig. 2(a) TEM image of pure ZnO sample.

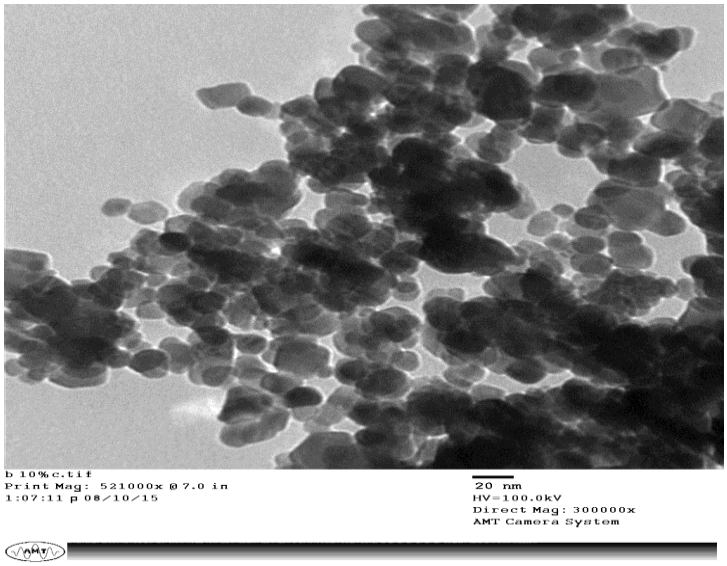

Fig. 2(b) TEM images of 10% Cr doped ZnO sample.

c. Optical study

The UV−visible was used to investigate the band gaps of pure and the Cr-doped ZnO samples. The optical absorption spectra of pure and Cr doped ZnO nanoparticles in the range of 800 nm to 200 nm was depicts in figure 3. From figure, it clearly shows that the absorption edge shift to words the longer wavelengths as Cr doping is increased. The direct band gap energy for the prepared samples are determined by fitting the absorption data to the direct transition equation

$$\alpha h\nu = A\,(h\nu - E_g)^{1/2} \qquad (8)$$

Specially, with n =1/2, a good linearity has been observed for the direct allowed transition, the most preferable one in the system studied. The exact value of band gap is determined by extrapolating the straight line portion of $(\alpha h\nu)^2$ vs hν to the x-axis. The direct band gap energy is found to be 3.06eV for pure, 2.92 for 5% Cr and 2.78 eV for 10% Cr doped ZnO nanoparticles. It was observed that the Cr affect the energy band gap. Similar result have reported by Kayani et al. [19] on Cr doped ZnO nanocrystals. Kumar et al. [20] have investigated the band gap decreases with higher concentration of Cr doping. This result is in agreement with our result.

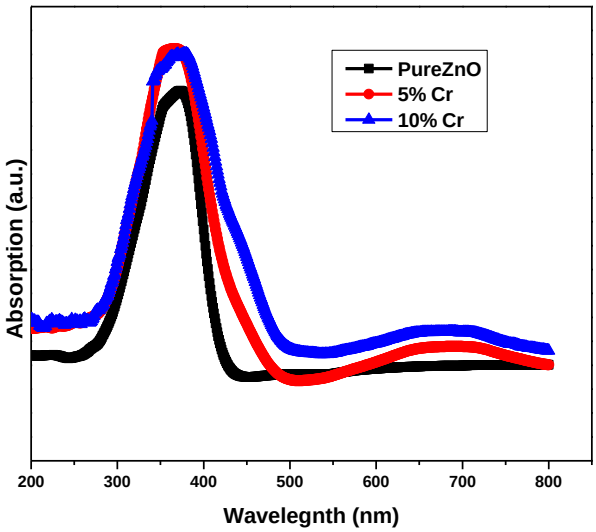

Fig. 3 UV-Vis spectra of pure and Cr doped ZnO nanoparticles.

The change of energy band gap of the materials was depends on sizes of nanomaterials using quantum effect [21]. In our case, the energy band gap is not depending on average crystallite size of the prepared samples. Because, the average crystallite sizes of $Zn_{1-x}Cr_xO$ nanoparticles were larger than that the exciton Bohr radius (ZnO – 1.8 nm). So that, the energy band gap decreases in 3.06 to 2.78 eV with the Cr content. This band gap narrowing of transition metal doped II-IV semiconductor is likely to be interpreted in terms of sp-d spin exchange interactions between the conduction band electrons and the localized d electrons of transition metals ions Cr. This is a typical characteristic of nano-sized materials, so the co-precipitation derived Cr doped ZnO nanoparticles will take on excellent properties in practical applications.

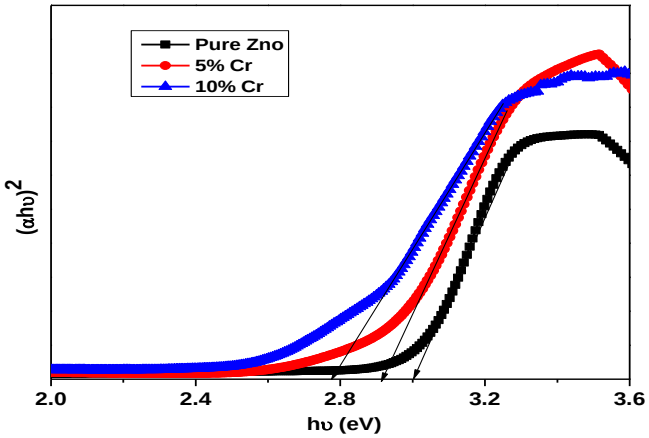

Fig 4. $(\alpha h\nu)^2$ Vs hν of pure and Cr doped ZnO nanoparticles.

IV. CONCLUSIONS

In summary, the nanoparticles of pure and Cr doped ZnO were grown by co-precipitation route. The XRD patterns confirm that prepared samples have hexagonal crystal structure. TEM images were demonstrated the formation of nanoparticles in the range of 17-23 nm. The size and strain contribution to line broadening were analyzed, it was observed that the strain value increased but particle size decreased as Cr doping was increased. Optical measurement reveals the optical energy band gap decreases with a Cr doping of ZnO nanoparticles, with slight enhancement of optical band gap due to Cr doping. The structural,

morphological and optical properties of pure and Cr doped ZnO nanoparticles will play an important role in promoting its practical application in the future.

References

1. H. Ohno, D. Chiba, F. Mutsukura, T. Omiya, E. Abe, T. Dietl, Y. Ohno, K. Ohtani, Nature (London), 408 (2000) 944.
2. J.R. Harbour, M.L. Hair, J. Phys. Chem. 83 652(1979).
3. P. Mitra, A. Chatterjee, H. Maiti, Mater. Lett. 35 (1998) 33.
4. T.K. Gupta, J. Am. Ceram. Soc. 73 (1990) 1817.
5. A.V. Dijken, E.A. Mulenkamp, D. Vanmaekelbergh, A. Meijerink, J. Lumin. 90 (2000) 123.
6. J. B. Baxter, A. M. Walker, K. Van Ommering, E. S. Aydil, Nanotechology 17 (2006) S304.
7. J. Suehiro, N. Nakagawa, S. Hidaka, M Ueda, K. Imasaka, M. Higashihata, T. Okada, M. Hara, Nanotechnology 17 (2006) 2567.
8. B.K. Roberts, A.B. Pakhomov, V.S. Shutthanandan, K.M. Krishnan, J. Appl. P 97 (2005) 10D310.
9. H. K. Park, D. K. Kirn, C. H. Kirn, J. Am. Ceram. Soc. 80, 743 (1992).
10. T. T. Kodas, Adv. Mater. 6, 180 (1989).
11. B. P. Zhang, N. Y. Binh, K. Wakatsuki, Y. Segawa, Y. Yamada, N. Usami, M. Kawasaki, H. Koinuma, J. Phys. Chem. B 108, 10899 (2004).
12. G. Z. Shen, Y. Bando, Ch.J. Lee, J. Phys. Chem. B 109, 10578 (2005).
13. S. I. Hirano, Ceram. Bull. 66, 1342 (1987).
14. H. Zhang, D. R. Yang, D. S. Li, X. Y. Ma, S. Z. Li, D. L. Que, Cryst. Growth Des.2, 547 (2005).
15. B. Liu, H.C. Zeng, Langmuir 20, 4196 (2004).
16. Wilson, A.C.J.: X-ray Optics. UK, London (1949).
17. A. R. Stokes, A. J. C. Wilson, Proc. Phys. Soc. (London,U. K.) 56 (1944) 174–181.
18. D. Balzar, N. Audebrand, M. R. Daymond, A. Fitch, A. Hewat, J. I. Langford, A. Le Bail, D. Louër, O. Masson, C. N. McCowan, N. C. Popa, P. W. Stephens, B. H. Toby, J. Appl. Crystallogr. 37 (2004) 911–924.
19. Z.N. Kayani, M. Siddia, S. Rianz, S. Naseem, Materials Research Express, 4 (2017) 096403.
20. S. Kumar, N. Tiwari, S.N. Jha, S. Chatterjee, D. Bhattacharyya, A.K. Gosh, RSC. Adv., 6 (2016) 107816-107828.
21. O. Lupan, T. Pauporte, L. Chow, B. Viana, F. Pelle, L.K. Ono, B.R. Cuenya, H. Heinrich, Appl. Surf. Sci. 256, 1895-1907 (2010).